HHS Public Access

Author manuscript

Immunol Cell Biol. Author manuscript; available in PMC 2018 March 11.

Published in final edited form as:

Immunol Cell Biol. 2017 November ; 95(10): 933–942. doi:10.1038/icb.2017.74.

A key role for IL-7R in the generation of microenvironments required for thymic dendritic cells

Amanda J. Moore[1,2,*], **Tracy S.H. In**[1,2,*], **Ashton Trotman-Grant**[1,2], **Kogulan Yoganathan**[1,2], **Bertrand Montpellier**[2,3], **Cynthia J. Guidos**[2,3], **Juan Carlos Zúñiga-Pflücker**[1,2], and **Michele K. Anderson**[1,2,4]

[1]Biological Sciences, Sunnybrook Research Institute, Hospital for Sick Children Research Institute, Toronto, ON, Canada

[2]Department of Immunology, University of Toronto, Hospital for Sick Children Research Institute, Toronto, ON, Canada

[3]Program in Developmental and Stem Cell Biology, Hospital for Sick Children Research Institute, Toronto, ON, Canada

Abstract

Interleukin-7 receptor (IL-7R) signaling is critical for multiple stages of T-cell development, but a role in the establishment of the mature thymic architecture needed for T-cell development and thymocyte selection has not been established. Crosstalk signals between developing thymocytes and thymic epithelial cell (TEC) precursors are critical for their differentiation into cortical TECs (cTECs) and medullary TECs (mTECs). Additionally, mTECs-derived factors have been implicated in the recruitment of thymic dendritic cells (DCs) and intrathymic DC development. We therefore examined corticomedullary structure and DC populations in the thymus of *Il7r*$^{-/-}$ mice. Analysis of TEC phenotype and spatial organization revealed a striking shift in the mTEC to cTEC ratio, accompanied by disorganized corticomedullary structure. Several of the thymic subsets known to have DC potential were nearly absent, accompanied by reductions in DC cell numbers. We also examined chemokine expression in the *Il7r*$^{-/-}$ thymus, and found a significant decrease in mTEC-derived CCR7 ligand expression, and high levels of cTEC-derived chemokines, including CCL25 and CXCL12. Although splenic DCs were similarly affected, bone marrow precursors capable of giving rise to DCs were unperturbed. Finally, bone marrow chimeras showed that there was no intrinsic need for IL-7R signaling in the development or recruitment of thymic

[4]Corresponding author: Michele K. Anderson, Sunnybrook Research Institute, 2075 Bayview Avenue, Room M7-615, Toronto, ON, M4N 3M5. Phone: 416-480-6138. Fax: 416-480-4375. manderso@sri.utoronto.ca.

[*]These authors contributed equally to this work

AUTHOR CONTRIBUTIONS

AJM, MKA, CJG, and JCZP conceived the project, designed experiments, and analyzed and interpreted the results; AJM, TSHI, and ATG performed most experiments; KY and BM assisted in experiments; AJM and MKA wrote the manuscript, and all other authors provided editorial advice.

CONFLICT OF INTEREST

The authors declare no conflict of interest.

The Supplementary Information that accompanies this paper is available on the Immunology and Cell Biology website (http://www.nature.com/icb).

DCs, but that the provision of WT progenitors enhanced reconstitution of thymic DCs from *Il7r*$^{-/-}$ progenitors. Our results are therefore supportive of a model in which *Il7r*-dependent cells are required to set up the microenvironments that allow accumulation of thymic DCs.

Introduction

Discrimination of self from non-self is the fundamental basis of immunity. In the adaptive immune system, this process depends heavily on the deletion of potentially autoreactive T-cells in the thymus. The thymus is roughly divided into regions of cortical thymic epithelial cells (cTECs) and medullary thymic epithelial cells (mTECs), linked by a corticomedullary junction (CMJ). These microenvironments provide unique niches that support successive stages of T-cell development, as well as recruitment of thymic seeding progenitors and dendritic cells (DCs)[1]. mTECs collaborate with thymic DCs to delete potentially autoreactive T-cells, or to re-direct them to the T-regulatory lineage[2, 3]. Several types of DCs are present in the thymus. CD11b^{-} conventional DCs (cDCs), which represent the majority of thymic cDCs, can develop intrathymically[4–6], whereas CD11b^{+} cDCs and plasmacytoid DCs (pDCs) are thought to be recruited to the thymus by chemokines[7–9]. However, the orchestration of thymic DC development and recruitment within the corticomedullary territories is not well understood.

mTECs develop from bipotent TEC precursors that mature into either cTECs and mTECs during early fetal life. Later in ontogeny, mTECs can develop from cTEC-like precursors[10], indicating a concurrent upregulation of mTEC genes and downregulation of cTEC-specific genes at this developmental transition. TEC differentiation and maturation are highly dependent on bi-directional signaling between developing T-cells and TECs in a process termed thymic crosstalk[11]. mTEC emergence and maturation at E16 is regulated by RANK (Receptor Activator of Nuclear Factor κ B) ligand (RANKL)-expressing innate-like lymphoid cells (ILCs)[12] and Vγ5 dendritic epidermal T-cells (DETCs)[13]. In the adult thymus, CD4^{+} T-cells expressing RANKL and CD40L provide signals for mTEC maturation[12, 14]. mTEC maturation results in the upregulation of autoimmune regulator (AIRE), which is necessary for negative selection and associated with chemokine-mediated recruitment of cells to the medulla[15]. The development of DETCs and ILCs is dependent on IL-7R signaling[16–19], but the consequences of IL-7R deficiency on TEC development and corticomedullary structure have not been investigated.

In addition to mediating T-cell development, TECs also play roles in the recruitment and localization of thymic DCs. Several subsets of CD4^{-}CD8^{-} double negative (DN) precursors in the thymus have been shown to have the capacity to give rise to DCs, including DN1a/b (ETPs, early thymic precursors), DN1c, DN1d, DN1e, and DN2a cells[5, 6, 20, 21]. ETPs and DN2a cells have strong T-cell potential, suggesting that some thymic DCs may arise from precursors which can respond to divergent signals within the thymic microenvironment to adopt either a T-cell or a DC lineage fate[22]. One such cue could be Notch signaling, which promotes the T-cell fate and inhibits the DC fate[6, 23, 24]. In this respect, the medulla provides a more conducive environment for intrathymic DC development than the cortex, in that it contains lower levels of Delta-like (Dll) Notch ligands[24, 25]. However, the potential impact a

disorganized thymic structure on thymic DC development and recruitment has not been well explored.

Most thymic DCs are specifically concentrated within and near the medulla[26, 27]. The recruitment of extrathymically-derived DCs to the thymus is dependent in part on chemokines, including CCL19 and CCL21[28–30]. CCL19 and CCL21 are ligands for CCR7, which is expressed on all thymic DCs[6]. CCL25, CXCL12, and CCL2 are cTEC-derived chemokines that can recruit distinct subsets of DCs from the periphery. Furthermore, XCR1-expressing thymic DCs require the mTEC-derived chemokine XCL1 to localize to the medulla[27]. The question therefore arises as to whether recruitment of DCs to the thymus would be impacted by disturbances in TEC development and corticomedullary structure.

Given that the mediators of thymic crosstalk are dependent on IL-7R signaling, we examined TECs, thymic structure, and DC populations in *Il7r*$^{-/-}$ mice. We found that *Il7r*$^{-/-}$ mice exhibited a striking decrease in the percentages of mTECs, accompanied by disorganized corticomedullary structure. The *Il7r*$^{-/-}$ thymus also exhibited a dysregulation of TEC-mediated chemokine production and MHC Class II (MHC II) expression. Thymic DCs exhibited decreased cellularity that spanned all three major subsets, and a depletion of putative intrathymic DC precursors. Mixed bone marrow chimeras were consistent with a cell-extrinsic role for *Ilr7* in DC population of the thymus. Taken together, our results suggest that IL-7R signaling is critical for generating the thymic microenvironments conducive to accumulation of DCs in the thymus.

RESULTS

Disruption in cTEC and mTEC ratios and cTEC phenotypes in Il7r$^{-/-}$ mice

To assess whether TEC development and corticomedullary structure were impacted by a loss of *Il7r*-dependent cells, we examined the presence and abundance of cTECs and mTECs in the *Il7r*$^{-/-}$ thymus by flow cytometry. Our results revealed an approximate 5-fold enrichment of the frequency of TECs (EpCAM^{+}) in the *Il7r*$^{-/-}$ thymus as compare with the WT thymus (Fig. 1A), due to a significant decrease in thymocyte cell numbers[19]. The majority of the TECs in the WT thymus were UEA-1^{+}Ly51^{-} mTECs, with approximately half of those expressing high levels of MHC II (Fig. 1B, D). By contrast, the vast majority of TECs in the *Il7r*$^{-/-}$ thymus were Ly51^{+}UEA-1^{-} cTECs (Fig. 1B), indicating a severe block in the generation of mTECs. However, the few *Il7r*$^{-/-}$ mTECs that were present exhibited the same proportion of immature (MHC II^{lo}) to mature (MHC II^{hi}) mTECs as the WT. Surprisingly, nearly all of the *Il7r*$^{-/-}$ cTECs were MHC II^{hi}, in contrast with the MHC II^{lo} status of the majority of the WT cTECs (Fig. 1C). cTECs are largely MHC II^{hi} between E15.5 and about a week after birth, whereas they are mostly MHC II^{lo} in the adult thymus (Fig. 1B)[31]. Therefore, the preponderance of MHC II^{hi} cTECs in the *Il7r*$^{-/-}$ thymus suggests a partial block in the cTEC MHC II^{hi} to mTEC MHC II^{hi} developmental transition.

To further characterize the *Il7r*$^{-/-}$ TECs, we measured the levels of the expression of key TEC genes in whole unfractionated thymus by qRT-PCR (Fig. 1E). β5t (*Psmb11*) and cytokeratin 8 (K8) are expressed by cTECs, whereas cytokeratin 5 (K5) is preferentially expressed by mTECs[32]. High levels of MHC II and AIRE indicate mTEC maturity. The

Il7r$^{-/-}$ thymus had higher levels of β5t, *K8*, *K5*, and *MHC II* mRNA than WT thymus, consistent with the higher ratio of TECs to thymocytes, and with the high expression of MHC II on the *Il7r*$^{-/-}$ cTECs (Fig. 1C). Strikingly, however, *AIRE* mRNA levels were significantly lower in the *Il7r*$^{-/-}$ thymus compared to the WT thymus, providing evidence that very few fully mature mTECs were present.

Disorganized thymic architecture and DC localization in Il7r$^{-/-}$ mice

We next examined corticomedullary structure of *Il7r*$^{-/-}$ thymus using immunofluorescent staining for K8 and K5. Tiled sections revealed distinct cortical and medullary regions in the WT thymus, identified by K8^{+} and K5^{+} staining, respectively, along with DCs (CD11c^{+}), which were primarily located in the medullary regions (Fig. 2A). By contrast, there were no clear medullary structures in the *Il7r*$^{-/-}$ thymus, and most of the K8^{+} TECs co-stained with K5, suggestive of developmental immaturity[33, 34]. K8^{+}K5^{+} cells were also present in small numbers in the WT medulla and enriched at the corticomedullary junction, as expected[33, 35, 36]. Thymic DCs cells were clearly detectable in the WT thymus, localized primarily to the medulla, but were sparse in the *Il7r*$^{-/-}$ thymus (Fig. 2B). Thus, our results reveal a disruption of TEC subset distribution, cTEC features, and corticomedullary thymic structure in *Il7r*$^{-/-}$ mice, as well as a decrease in thymic DCs.

Decreases in numbers of all three thymic DC subsets in the Il7r$^{-/-}$ mice

We next evaluated the proportions of these three DC subsets in WT and *Il7r*$^{-/-}$ mice by flow cytometry. Thymic DCs were identified by first excluding cells expressing CD3, TCRγδ, TCRβ, CD19, NK1.1, F4/80, and Ter119 lineage (Lin) markers, followed by gating on CD45^{+}Lin^{-} cells to examine pDCs (CD11c^{int} PDCA-1^{+}) and cDCs (CD11c^{high}PDCA-1^{-}) (Fig. 3A). cDCs were further subdivided based on the expression of CD11b into CD11b^{-} cDCs (CD11c^{+}PDCA-1^{-}CD11b^{-}) and CD11b^{+} cDCs (CD11c^{+} PDCA-1^{-}CD11b^{+}) (Fig. 3B). The ratios of DCs to total thymic cell number were higher in the *Il7r*$^{-/-}$ mice (Fig. 3A), due to the severe decrease in thymocyte cellularity of approximately 100-fold. However, the total DC numbers were in the *Il7r*$^{-/-}$ thymus were decreased by about 25-fold (Fig. 3C). This was true across all three major thymic DC subsets, and no notable differences were apparent between the proportions of the three DC subsets in the WT as compared with the *Il7r*$^{-/-}$ thymus (Fig. 3D). Therefore, in terms of numbers, thymic DCs were not spared from the impact of *Il7r* deficiency on the thymus.

Loss of potential intrathymic DC precursors in Il7r$^{-/-}$ mice

The low numbers of thymic DCs in *Il7r*$^{-/-}$ mice could have been due to several factors: 1) a loss of DC progenitors within the thymus, 2) a failure of DCs to migrate to the thymus, and/or 3) a loss of DCs or their progenitors prior to entry into the thymus. A simple lack of space in the smaller thymus could also potentially account for the DC number decreases, but the changes in the cTEC to mTEC ratio showed that *Il7r*$^{-/-}$ thymic “space” was altered in character as well as size. We therefore assessed other potential mechanisms for DC paucity in the *Il7r*$^{-/-}$ thymus. We first examined the status of DN1 subsets, all of which have been shown to have some DC potential[5, 6, 20] within the *Il7r*$^{-/-}$ thymus (Fig. S1A). There was a partial increase in DN2 and decrease in DN3 cell frequencies among the DN (CD4^{-}CD8^{-}Lin^{-}) compartment in the *Il7r*$^{-/-}$ thymus, as previously reported[19, 37]. However,

the *Il7r*$^{-/-}$ thymus also displayed a near absence of ETPs, DN1c, and DN1d cells. To further define the DC potential of these subsets, we sorted them from WT thymus, and placed them into co-culture with OP9-DL1 cells supplemented with SCF, Flt3L, and IL-7 for four days. OP9-DL1 co-culture mimics the thymic environment by providing Notch ligands to precursor cells[38]. These DN1 subsets have been previously assayed for T cell, B cell, and NK potential[22], but they have not been tested for DC potential under these conditions. In this context, ETPs clearly had the most DC potential, with very few CD11c^{+} cells detected in cultures containing DN1c, DN1d, or DN1e cells (Fig. S1B). These data suggest that the ETP subset contains precursors with DC potential in the presence of Notch ligands, and their depletion in the *Il7r*$^{-/-}$ thymus suggests one mechanism by which intrathymic DC development could be impacted by the lack of *Il7r*.

Decreased CCR7 ligand expression in the Il7r$^{-/-}$ thymus

Whereas CD11b^{-} thymic DCs can develop within the thymus, CD11b^{+} cDC and pDCs are thought to migrate to the thymus from the periphery[7–9]. Migration of mature DCs from the periphery to the thymus is directed by chemokines produced by TECs[39]. We therefore measured the mRNA expression of six TEC-derived chemokines in WT and *Il7r*$^{-/-}$ whole thymus. We normalized the results to EpCAM mRNA levels, to account for the differences in TEC abundance (Fig. 4A). *CCL21*, *CCL19*, and *XCL1* expression were significantly lower in the *Il7r*$^{-/-}$ thymus than WT thymus, consistent with the defect in mTEC development. By contrast, *CXCL12* and *CCL25* transcripts were markedly higher in *Il7r*$^{-/-}$ thymus than WT thymus. *CCL2* expression was not significantly different. The paucity of CCR7 ligands in the *Il7r*$^{-/-}$ thymus suggests that defective recruitment and retention could account in part for the decreased numbers of CD11b^{+} cDCs and pDCs. However, the high levels of *CCL25* and *CXCL12* could potentially mediate recruitment of pDCs and CD11b^{+} cDCs, respectively.

Increased levels of chemokine expression in Il7r$^{-/-}$ cTECs relative to WT cTECs

To assess whether chemokine expression changes in the *Il7r*$^{-/-}$ thymus were due to the ratio of cTECs to mTECs, or due to alterations within the TEC subsets, we sorted cTECs and mTECs from WT and *Il7r*$^{-/-}$ thymus and measured chemokine mRNA expression by qRT-PCR (Fig. 4B). The amounts of *CCL19* produced by WT versus *Il7r*$^{-/-}$ mTECs were roughly the same whereas levels of CCL21 were lower in *Il7r*$^{-/-}$ mTECs. Surprisingly, *CCL21* was highly elevated in *Il7r*$^{-/-}$ cTECs, in spite of its decrease in mTECs, and in the whole thymus of *Il7r*$^{-/-}$ mice relative to WT. These data suggest that a disruption in a non-TEC population, such as fibroblasts or endothelial cells, may have been responsible for the decrease in *CCL21* mRNA expression observed in the unfractionated *Il7r*$^{-/-}$ thymus.

The chemokine expression profiles we obtained from WT cTECs and mTECs corresponded well to the WT TEC subset data in the Immunological Genome Project (ImmGen, www.immgen.org) dataset[40] (Fig. S2). Interestingly, the higher levels of chemokine expression in WT MHC II^{hi} cTECs correspond well to their elevated levels in *Il7r*$^{-/-}$ cTECs, which express more MHC II than their WT counterparts (Fig. 1C). mTECs in the *Il7r*$^{-/-}$ thymus also expressed higher levels of the normally cTEC-derived chemokines, suggesting

that they may have failed to fully repress these genes during development through a cTEC-like progenitor in the absence of IL-7R signaling.

Splenic DCs are decreased in Il7r$^{-/-}$ mice

Another factor that could contribute to the decrease in DCs in the *Il7r*$^{-/-}$ thymus would be a defect in DCs and/or their precursors prior to thymic entry. To assess this possibility, we analyzed splenic DCs in WT and *Il7r*$^{-/-}$ mice (Fig. S3A, B). The total numbers of DCs were decreased in the *Il7r*$^{-/-}$ spleen (Fig. S3C), although not to the same extent as that observed in the thymus. Interestingly, the proportions of DC subsets in the *Il7r*$^{-/-}$ spleen were not notably different from those in WT spleen, mirroring what we observed in the thymus (Fig. S3D). Since both splenic and thymic DCs were impacted by *Il7r*-deficiency, we asked whether there was a defect in a common DC precursor outside the thymus by examining bone marrow precursor subsets. CLPs and B-lineage cells were mostly absent in *Il7r*$^{-/-}$ mice, as expected[41]. However, CMPs, LSKs, LMPPs were all detectable to similar degrees, in agreement with previously published results (data not shown)[42]. These results suggest that rather than revealing a common extrathymic defect in DC precursors, the decrease in splenic DCs in *Il7r*$^{-/-}$ mice may reflect independent microenvironmental defects in the spleen that occur in parallel to the thymus.

Mixed bone marrow chimeras reveal a non-cell intrinsic requirement for IL-7R signaling in thymic DC generation

To assess the extent to which the decrease in thymic and splenic DCs in the *Il7r*$^{-/-}$ mice resulted from a cell-intrinsic DC defect versus cell-extrinsic defects, we performed mixed bone marrow chimeras. Equal numbers of CD45.1^{+} C57Bl/6 WT (“WT donor”) BM and CD45.2^{+} *Il7r*$^{-/-}$ (“KO donor”) BM cells were injected into lethally irradiated C57BL/6 CD45.2^{+} × C57BL/6 CD45.1^{+} F1 (“Host”) recipient mice, and the thymus and spleen were analyzed by flow cytometry after 21 days. Since previous studies have shown that the lifespan of DCs within lymphoid organs ranges from one to nine days[43], the DCs that we observed three weeks after injection would have developed from donor precursors rather than representing mature DCs present in the bone marrow preparation prior to injection. In this competitive approach, development of WT thymocytes could potentially restore thymic architecture after irradiation. As expected, nearly all of the thymocytes in the mixed chimera were derived from the WT donor cells (Fig. 5A), due to the intrinsic need for IL-7R signaling at early stages of T-cell development[37]. *Il7r*$^{-/-}$ bone marrow also contributed less to overall splenocyte reconstitution than WT bone marrow, consistent with defects in both B-cell and T-cell development, although the defect was less drastic. By contrast, we observed equal contribution from WT and *Il7r*$^{-/-}$ donors among both splenic and thymic DCs (Fig. 5B), with no skewing of the DC subsets (Fig. 5C). These results indicate that thymic DCs do not have an intrinsic need for IL-7R signaling.

WT bone marrow rescues Il7r$^{-/-}$ thymic DC numbers in mixed chimeras

To evaluate whether the presence of WT thymocytes restored the environment needed for thymic DC accumulation, we conducted single chimeras alongside mixed chimeras and examined DC subsets and numbers. CD45.1^{+} C57Bl/6 WT (“WT donor”) whole bone marrow, CD45.2^{+} *Il7r*$^{-/-}$ (“KO donor”) whole bone marrow, or a 1:1 mix, were injected into

lethally irradiated C57BL/6 CD45.2$^+$ × C57BL6 CD45.1$^+$ F1 (“Host”) recipient mice, and the thymuses were analyzed by manual counting and flow cytometry after 21 days (Fig. 6 and data not shown). The total numbers of thymic CD45$^+$ cells derived from *Il7r*$^{-/-}$ donors were greatly decreased relative to WT donors, in the both in the single and mixed chimeras (Fig. 6A), whereas the percentages of DCs within each donor population was much higher (Fig. 6B). However, the absolute numbers of *Il7r*$^{-/-}$ donor-derived DCs in the *Il7r*$^{-/-}$ single chimeras were much lower than the numbers of WT donor-derived DCs in the WT single chimeras, suggesting that the thymus reconstituted with *Il7r*$^{-/-}$ cells alone created an inhospitable environment for DCs (Fig. 6C). This was true of all three DC subsets, and there was no significant difference in their proportions (not shown). By contrast, *Il7r*$^{-/-}$ DC cell numbers were largely rescued in the mixed chimera, such that the approximately equal contribution of *Il7r*$^{-/-}$ and WT DCs restored total donor DC numbers to roughly the same numbers of DCs that were present in the single WT chimeras (Fig. 6D).

DISCUSSION

Although thymic-stromal crosstalk is known to be necessary to create an environment conducive to T-cell development, less is known about how it impacts thymic DCs. Here we have shown that *Il7r*$^{-/-}$ mice exhibit severe defects in thymic corticomedullary structure and mTEC development, and that they have a paucity of DCs in the thymus. We investigated a variety of potential mechanisms for the DC defect, and found evidence for a decrease in potential intrathymic DC precursors, and alterations in chemokines that enable DC migration to the thymus. Our single and mixed chimera data indicated that the failure of DCs to populate the thymus in *Il7r*$^{-/-}$ mice did not reflect an intrinsic need for IL-7R signaling in DCs or their pre-thymic precursors, but was rather caused by a lack of proper intrathymic environmental cues. Altogether, our results resolve a long-standing conflict about the nature of the role of *Il7r* in thymic DC development, and reveal a new role for *Il7r*-dependent crosstalk in TEC development.

Thymic crosstalk between thymocytes and TECs is essential for mTEC maturation and the generation of medullary structures[44, 45]. In line with our hypothesis that the primary defects in TECs and thymic DCs are cell-extrinsic, it is clear that many of the phenotypes we observed in the *Il7r*$^{-/-}$ mice manifest in cells that do not express *Il7r*, including TECs and cDCs. Elegant fate mapping experiments in which YFP was driven under the control of the *Il7r* regulatory regions clearly showed that although most pDCs in spleen and thymus were derived through an *Il7r*-expressing intermediate, cDCs were not[46]. In our study, the proportion of pDCs among total DCs was similar in the spleen and thymus of *Il7r*$^{-/-}$ relative to WT mice, and the chimera data indicates that suggesting that *Il7r*$^{-/-}$ pDCs are not intrinsically dependent on IL-7R signaling.

One of the most striking findings in this study is the severe impact of *Il7r* loss on TECs. This is most likely due to a failure of crosstalk normally provided by *Il7r*-dependent thymocytes or ILCs. An absence of DETCs is not sufficient to drive this defect, as we found that mature TCRδ$^{-/-}$ mice had normal thymic architecture, cell numbers, and DCs (not shown). CD4$^+$ SP cells, which can also supply crosstalk signals to TECs, are abundant in the *Il7r*$^{-/-}$ thymus[19]. However, our data suggest that they may be defective in their ability to support

the generation of mTECs. The mechanistic basis for a failure in thymic crosstalk between *Il7r*$^{-/-}$ thymocytes and TECs has yet to be determined, but previous studies suggest a role for IL-7R signaling in inducing the expression of TNF receptor and ligand family members that are involved in thymic crosstalk[44, 47]. One prime candidate is LTβR, since TECs from *Ltbr*$^{-/-}$ mice are deficient in their ability to make CCL19, but competent to make CCL21, CCL25, and CXCL12, reminiscent of the *Il7r*$^{-/-}$ TEC gene expression profile[48].

Another population that was clearly impacted by the absence of *Il7r* was ETPs. ETPs, which do not express easily detectable levels of *Il7r*, can arise from *Il7r*-dependent CLPs, but can also arise in their absence[22, 49]. In the *Il7r* fate mapping study, 85% of ETPs were labeled with a history of *Il7r* expression, whereas 15% were not[46]. Therefore, the near absence of ETPs we observed in the *Il7r*$^{-/-}$ thymus was not solely due to a defect in CLP-like progenitors. Furthermore, ETPs are severely depleted in the *Rag2*$^{-/-}$ thymus ([50] and unpublished observations), which also have disorganized thymic architecture, suggesting that their recruitment or maintenance is faulty without the proper microenvironmental conditions. ETPs are also depleted in the *Ltbr*$^{-/-}$ thymus[48], further implicating this pathway in the defects in *Il7r*$^{-/-}$ thymic structure.

Whereas DN1 subsets can give rise to DCs within the thymus, thymic pDCs and CD11b^{+} cDCs are thought to be largely recruited from outside the thymus by TEC-derived chemokines[7–9] Our results show that CCL19 and CCL21, which attract and maintain CCR7-expressing cells, including ETPs and DCs, are decreased in the thymus as a whole. However, *CXCL2* and *CCL25* were expressed at high levels, consistent with the high percentage of MHC II^{hi} cTECs in the *Il7r*$^{-/-}$ thymus, suggesting an intact mechanism for recruitment of CCR9^{+} pDCs and CXCR4^{+} CD11b^{+} cDCs. Furthermore, while CCL19 expression was clearly limited to WT and *Il7r*$^{-/-}$ mTECs, CCL21 was expressed in both WT and *Il7r*$^{-/-}$ cTECs as well as mTECs, at reasonably high levels, providing an additional mechanism for recruitment of all three DC subsets. Therefore, retention or homeostasis of DCs is more likely to account for the defects in thymic pDC and CD11b^{+} cDC cell number than a defect in the initial recruitment of DC or their precursors to the *Il7r*$^{-/-}$ thymus.

Interestingly, there is a drastic reduction in thymic DCs in patients with primary immunodeficiencies[51]. In these studies, patients that manifested a block in T-cell development also displayed a defect in corticomedullary structure and a concurrent decrease in thymic DCs, whereas those that maintained corticomedullary structure also retained thymic DCs. Furthermore, there is a clear connection between primary immunodeficiencies and autoimmune diseases in humans, indicating a failure of central tolerance that could be due in part to the loss of thymic DCs[52]. Therefore, thymocyte-TEC crosstalk and corticomedullary structure appear to be essential for thymic DCs in humans as well as mice.

Taken together, our studies indicate that a loss of *Il7r*-dependent cells results in an inverted ratio of cTECs to mTECs, and also adversely impacts the accumulation of all three subsets of thymic DCs. The low numbers of all three DC subsets suggests that there may be a problem with overall DC retention or homeostasis Nonetheless, the lack of thymic pDCs and CD11b^{+} DCs are linked by a decrease in mTEC-derived CCL19, and the defect in thymic CD11b^{-} DCs may be due at least in part to the loss of DN1 subsets that could act as

intrathymic DC precursors. Importantly, our bone marrow chimera experiments provide evidence that the primary defects in the DC compartment of the *Il7r*$^{-/-}$ thymus are cell extrinsic. A role for *Il7r*-dependent hematopoietic cells in creating a DC-hospitable environment is supported by our observation that the restoration of WT thymocytes, overall thymus cellularity, and corticomedullary structure permitted *Il7r*$^{-/-}$ precursors to develop into DCs and accumulate in the thymus equally as well as WT precursors. Thus, our work has uncovered a requirement for IL-7R signaling in the complex network of cellular interactions required to create a thymic microenvironment that can support thymic DCs.

Methods

Animals

C57Bl/6 wildtype (WT) mice, CD45.1^{+} WT mice (Charles River, Charles River: Ly5Mouse/B6.SJL-PtprcaPepcb/BoyCrl) and *Il7r*^{tm1Imx}/*Il7r*^{tm1Imx} CD45.2^{+} mice (referred to as *Il7r*$^{-/-}$ mice, Jackson Laboratories) were maintained at the Sunnybrook Research Institute (SRI), Toronto, Ontario, Canada. All animal protocols were approved by the SRI animal care committee. Mice aged 4.5–6 weeks old were used for *ex vivo* analysis of T cells and thymic DCs. F1 progeny of CD45.2^{+} C57Bl/6 and CD45.1^{+} C57Bl/6 parents, aged 4.5–6 weeks old, were used as recipients for bone marrow (BM) chimera and competitive BM reconstitution experiments. Mice aged 7–12 weeks old were used for bone marrow donor cells. Donor mice were aged-matched in each independent experiment, as were recipient mice.

Harvesting of thymic DCs and TECs for flow cytometry

DCs and TECs were harvested from thymus by treatment with 2 mL of collagenase IV (0.1% m/v in PBS) and DNaseI (20 μg/mL in PBS; Life Technologies) for 10 minutes at 37 degrees C at 150 rpm, followed by a second round of collagenase IV/DnaseI digestion. Next, the homogenate was further digested twice with 2 mL collagenase dispase (0.12% m/v in PBS; Life Technologies) and 20 μg/mL DnaseI, at 37°C, 150 rpm. Thymic cells were obtained following two 10 minute incubations with 2 mL of 0.1% collagenase IV and two 10 minute incubations with 2 mL of 0.12% collagenase dispase. Remaining tissue was pushed through 40 μm pore nylon mesh (BD Biosciences) to obtain a single cell suspension of thymocytes, including TECs and DCs. Total cell counts were obtained using a hemocytometer.

Flow cytometry analysis

All samples were stained in HBSS, 0.5% BSA, 0.5 mM EDTA buffer at 4°C and were initially incubated with anti-FcγR antibodies to eliminate non-specific staining prior to antibody incubation. For ex vivo analysis of thymic DCs from WT versus *Il7r*$^{-/-}$ mice the following antibodies were used: anti-CD8 (PerCP); anti-CD11b (Alexa Fluor® 700); anti-PDCA-1 (PE); anti-CD11c (PECy7); anti-CD45 (APCCy7); Lineage (anti-CD3 (biotin); anti-TCRγδ (biotin); anti-TCRβ (biotin); anti-CD19 (biotin); anti-NK1.1 (biotin); anti-F4/80 (biotin), anti-Ter119 (biotin)) and streptavidin-eFluor® 450 (eBioscience, BD Biosciences, SRI Antibody Core Facility). TEC analysis was done with the following antibodies: anti-CD45 (APCeFluor®780); anti-EpCam (APC); anti-Ly51 (PE); anti-MHCII (FITC); anti-CD80 (PerCPeFluor®710); anti-UEA-1 (biotin) and streptavidin-PeCy7

(Vector Laboratories, eBioscience, BD Biosciences, SRI Antibody Core Facility). DAPI was used to exclude dead cells. *Il7r*$^{-/-}$ bone marrow chimera analysis was done using the following antibodies: anti-CD11c (PE); anti-CD8α (APC); anti-CD11b (Alexa Fluor® 700); anti-CD45.2 (APCCy7); anti-CD45.1 (PeCy7); Lineage (anti-CD3ε (biotin); anti-TCRγδ (biotin); anti-TCRβ (biotin) anti-CD19 (biotin); anti-NK1.1 (biotin), anti-F4/80 (biotin), anti-Ter119 (biotin) and streptavidin-eFluor® 450 (eBioscience, BD Biosciences, SRI Antibody Core Facility). DAPI was used to exclude dead cells. Following multiple washes with PBS, all samples were fixed with 1% m/v paraformaldehyde. Samples were run on an LSR II (BD Biosciences) and data was analyzed using FlowJo software (TreeStar).

Bone marrow Chimeras

For the WT versus *Il7r*$^{-/-}$ BM chimeras, 4.5–6 week old F1 (CD45.2^{+} C57Bl/6 × CD45.1^{+} C57Bl/6) mice were lethally irradiated with 950 cGy and injected intravenously via tail vein with whole BM. For single reconstitutions, either 20 × 10^{6} CD45.1^{+} WT BM or 20 × 10^{6} CD45.1^{+} WT BM were injected, whereas mixed BM hosts received a donor mixture of 20 × 10^{6} *Il7r*$^{-/-}$ BM and 20 × 10^{6} CD45.1^{+} WT BM. Mice were analyzed 3 weeks after injections.

Immunofluorescence microscopy

Thymic lobes were frozen in OCT prior to cutting 10 μm sections that were fixed in 2% paraformaldehyde, blocked with PBS/5% FBS/0.05% triton and stained with combinations of anti-CD11c (FITC); anti-cytokeratin-5/anti-rabbit (Cy5); and anti-cytokeratin-8/anti-rat Cy3 (antibodies obtained from BD Biosciences; Jackson Immunoresearch Laboratories, Vector Labs). Images were acquired and tiled with a Zeiss Axiovert Fluorescent Microscope.

Gene Expression Analysis

For whole thymus, samples were homogenized, and RNA was harvested using TRIzol according to manufacturer's instructions (Invitrogen). First-strand cDNA was generated using SuperScript III Reverse Transcriptase (Invitrogen). qRT-PCR was performed in triplicate on cDNA with gene-specific primers and iTaq Universal SYBR Green Supermix (Bio-Rad). Samples were run and data was analyzed using an Applied Biosystems Sequence Detection System 7000. Results were normalized to *GAPDH*, *β-actin* or *EpCAM* expression, and calculations of relative values (n) were performed using the delta Ct method, where n=1.9^(experimental Ct – normalization Ct). For analysis of gene expression in TEC subsets, cTECs and mTECs were sorted based on the cell surface expression of EpCAM and either Ly51 or UEA-1. First strand cDNA was generated from sorted cells and subjected to qRT-PCR as described above.

OP9-DL1 co-cultures

DN1 subsets were sorted from WT thymus according to the following parameters: CD45^{+}CD4^{-}CD8^{-}CD44^{+}CD25^{-} to identify DN1 cells, and then further gated according to expression of c-kit and CD24 to give DN1a/b (ETP; c-kit^{hi} CD24$^{-/int}$), DN1c (c-kit^{int} CD24^{hi}), DN1d (c-kit^{lo} CD24^{+}) and DN1e (c-kit^{lo} CD24^{-}) cells. Sorted subsets were placed on OP9-DL1 cells for four days in the presence of 5 ng/mL SCF, 10 ng/mL IL-7, and 10

ng/mL Flt3L as previously described[38]. Cultures were analyzed by flow cytometry for expression of CD11b and CD11c to identify DC lineage potential in the DN1 subsets.

Calculations and Statistics

Percentages of each DC subset among all DCs were calculated by dividing the number of each DC subset by the total number of DCs within the sample. The absolute cell number of each DC subset was calculated by multiplying the percentages by the total cellularity. Error bars represent standard error of the mean. Two-tailed unpaired t-tests were used to calculate *p* values for statistical significance; ***p<0.005, **p<0.01, *p<0.05, ns=non-significant.

Supplementary Material

Refer to Web version on PubMed Central for supplementary material.

Acknowledgments

We thank Maria Luisa Toribio (Madrid) for helpful discussions. We thank Oscar A. Aguilar (Toronto) for help with irradiations. We also appreciate the assistance of Christina Lee for intravenous injections and animal care, and Gisele Knowles, Courtney McIntosh, and Geneve Awong for microscopy guidance and flow cytometry expertise. Thanks are due also to the Sunnybrook Comparative Research Facility for excellent animal care. This work was supported by grants CIHRMOP 82861 to MKA, CIHRMOP 119538 and NIH-1P01AI102853-01 to JCZP, OGS to AJM, OGS to TSHI, CIHR MOP11530 to CJG; JCZP is supported by a Canada Research Chair in Developmental Immunology.

References

1. Anderson G, Takahama Y. Thymic epithelial cells: working class heroes for T cell development and repertoire selection. Trends Immunol. 2012; 33:256–263. [PubMed: 22591984]
2. Koble C, Kyewski B. The thymic medulla: a unique microenvironment for intercellular self-antigen transfer. J Exp Med. 2009; 206:1505–1513. [PubMed: 19564355]
3. Ouabed A, Hubert FX, Chabannes D, Gautreau L, Heslan M, Josien R. Differential control of T regulatory cell proliferation and suppressive activity by mature plasmacytoid versus conventional spleen dendritic cells. J Immunol. 2008; 180:5862–5870. [PubMed: 18424705]
4. Donskoy E, Goldschneider I. Two developmentally distinct populations of dendritic cells inhabit the adult mouse thymus: demonstration by differential importation of hematogenous precursors under steady state conditions. J Immunol. 2003; 170:3514–3521. [PubMed: 12646612]
5. Luche H, Ardouin L, Teo P, See P, Henri S, Merad M, et al. The earliest intrathymic precursors of CD8α(+) thymic dendritic cells correspond to myeloid-type double-negative 1c cells. Eur J Immunol. 2011; 41:2165–2175. [PubMed: 21630253]
6. Moore AJ, Sarmiento J, Mohtashami M, Braunstein M, Zuniga-Pflucker JC, Anderson MK. Transcriptional priming of intrathymic precursors for dendritic cell development. Development. 2012; 139:373–384. [PubMed: 22186727]
7. Proietto AI, van Dommelen S, Zhou P, Rizzitelli A, D'Amico A, Steptoe RJ, et al. Dendritic cells in the thymus contribute to T-regulatory cell induction. Proc Natl Acad Sci U S A. 2008; 105:19869–19874. [PubMed: 19073916]
8. Proietto AI, van Dommelen S, Wu L. The impact of circulating dendritic cells on the development and differentiation of thymocytes. Immunol Cell Biol. 2009; 87:39–45. [PubMed: 19048018]
9. Li J, Park J, Foss D, Goldschneider I. Thymus-homing peripheral dendritic cells constitute two of the three major subsets of dendritic cells in the steady-state thymus. J Exp Med. 2009; 206:607–622. [PubMed: 19273629]
10. Takahama Y, Ohigashi I, Baik S, Anderson G. Generation of diversity in thymic epithelial cells. Nat Rev Immunol. 2017; 17:295–305. [PubMed: 28317923]

11. Lopes N, Serge A, Ferrier P, Irla M. Thymic crosstalk coordinates medulla organization and T-cell tolerance induction. Front Immunol. 2015; 6:365. [PubMed: 26257733]
12. Rossi SW, Kim MY, Leibbrandt A, Parnell SM, Jenkinson WE, Glanville SH, et al. RANK signals from CD4(+)3(-) inducer cells regulate development of Aire-expressing epithelial cells in the thymic medulla. J Exp Med. 2007; 204:1267–1272. [PubMed: 17502664]
13. Roberts NA, White AJ, Jenkinson WE, Turchinovich G, Nakamura K, Withers DR, et al. Rank signaling links the development of invariant γδ T cell progenitors and Aire(+) medullary epithelium. Immunity. 2012; 36:427–437. [PubMed: 22425250]
14. Akiyama T, Shimo Y, Yanai H, Qin J, Ohshima D, Maruyama Y, et al. The tumor necrosis factor family receptors RANK and CD40 cooperatively establish the thymic medullary microenvironment and self-tolerance. Immunity. 2008; 29:423–437. [PubMed: 18799149]
15. Laan M, Peterson P. The many faces of aire in central tolerance. Front Immunol. 2013; 4:326. [PubMed: 24130560]
16. Kang J, Coles M. IL-7: the global builder of the innate lymphoid network and beyond, one niche at a time. Semin Immunol. 2012; 24:190–197. [PubMed: 22421575]
17. Maki K, Sunaga S, Komagata Y, Kodaira Y, Mabuchi A, Karasuyama H, et al. Interleukin 7 receptor-deficient mice lack gammadelta T cells. Proc Natl Acad Sci U S A. 1996; 93:7172–7177. [PubMed: 8692964]
18. Peschon JJ, Morrissey PJ, Grabstein KH, Ramsdell FJ, Maraskovsky E, Gliniak BC, et al. Early lymphocyte expansion is severely impaired in interleukin 7 receptor-deficient mice. J Exp Med. 1994; 180:1955–1960. [PubMed: 7964471]
19. Osborne LC, Dhanji S, Snow JW, Priatel JJ, Ma MC, Miners MJ, et al. Impaired CD8 T cell memory and CD4 T cell primary responses in IL-7R alpha mutant mice. J Exp Med. 2007; 204:619–631. [PubMed: 17325202]
20. Masuda K, Kakugawa K, Nakayama T, Minato N, Katsura Y, Kawamoto H. T cell lineage determination precedes the initiation of TCR beta gene rearrangement. J Immunol. 2007; 179:3699–3706. [PubMed: 17785806]
21. Li L, Leid M, Rothenberg EV. An early T cell lineage commitment checkpoint dependent on the transcription factor Bcl11b. Science. 2010; 329:89–93. [PubMed: 20595614]
22. Porritt HE, Rumfelt LL, Tabrizifard S, Schmitt TM, Zuniga-Pflucker JC, Petrie HT. Heterogeneity among DN1 prothymocytes reveals multiple progenitors with different capacities to generate T cell and non-T cell lineages. Immunity. 2004; 20:735–745. [PubMed: 15189738]
23. Feyerabend TB, Terszowski G, Tietz A, Blum C, Luche H, Gossler A, et al. Deletion of Notch1 converts pro-T cells to dendritic cells and promotes thymic B cells by cell-extrinsic and cell-intrinsic mechanisms. Immunity. 2009; 30:67–79. [PubMed: 19110448]
24. Mohtashami M, Shah DK, Nakase H, Kianizad K, Petrie HT, Zuniga-Pflucker JC. Direct comparison of Dll1- and Dll4-mediated Notch activation levels shows differential lymphomyeloid lineage commitment outcomes. J Immunol. 2010; 185:867–876. [PubMed: 20548034]
25. Koch U, Fiorini E, Benedito R, Besseyrias V, Schuster-Gossler K, Pierres M, et al. Delta-like 4 is the essential, nonredundant ligand for Notch1 during thymic T cell lineage commitment. J Exp Med. 2008; 205:2515–2523. [PubMed: 18824585]
26. Porritt HE, Gordon K, Petrie HT. Kinetics of steady-state differentiation and mapping of intrathymic-signaling environments by stem cell transplantation in nonirradiated mice. J Exp Med. 2003; 198:957–962. [PubMed: 12975459]
27. Lei Y, Ripen AM, Ishimaru N, Ohigashi I, Nagasawa T, Jeker LT, et al. Aire-dependent production of XCL1 mediates medullary accumulation of thymic dendritic cells and contributes to regulatory T cell development. J Exp Med. 2011; 208:383–394. [PubMed: 21300913]
28. Griffith AV, Fallahi M, Nakase H, Gosink M, Young B, Petrie HT. Spatial mapping of thymic stromal microenvironments reveals unique features influencing T lymphoid differentiation. Immunity. 2009; 31:999–1009. [PubMed: 20064453]
29. Campbell JJ, Pan J, Butcher EC. Cutting edge: developmental switches in chemokine responses during T cell maturation. J Immunol. 1999; 163:2353–2357. [PubMed: 10452965]
30. Kwan J, Killeen N. CCR7 directs the migration of thymocytes into the thymic medulla. J Immunol. 2004; 172:3999–4007. [PubMed: 15034011]

31. Brunk F, Michel C, Holland-Letz T, Slynko A, Kopp-Schneider A, Kyewski B, et al. Dissecting and modeling the emergent murine TEC compartment during ontogeny. Eur J Immunol. 2017; 47:1153–1159. [PubMed: 28439878]
32. Alves NL, Takahama Y, Ohigashi I, Ribeiro AR, Baik S, Anderson G, et al. Serial progression of cortical and medullary thymic epithelial microenvironments. Eur J Immunol. 2014; 44:16–22. [PubMed: 24214487]
33. Mayer CE, Zuklys S, Zhanybekova S, Ohigashi I, Teh HY, Sansom SN, et al. Dynamic spatio-temporal contribution of single β5t+ cortical epithelial precursors to the thymus medulla. Eur J Immunol. 2016; 46:846–856. [PubMed: 26694097]
34. Klug DB, Carter C, Crouch E, Roop D, Conti CJ, Richie ER. Interdependence of cortical thymic epithelial cell differentiation and T-lineage commitment. Proc Natl Acad Sci U S A. 1998; 95:11822–11827. [PubMed: 9751749]
35. Wong K, Lister NL, Barsanti M, Lim JM, Hammett MV, Khong DM, et al. Multilineage potential and self-renewal define an epithelial progenitor cell population in the adult thymus. Cell Rep. 2014; 8:1198–1209. [PubMed: 25131206]
36. Ohigashi I, Zuklys S, Sakata M, Mayer CE, Hamazaki Y, Minato N, et al. Adult thymic medullary epithelium is maintained and regenerated by lineage-restricted cells rather than bipotent progenitors. Cell Rep. 2015; 13:1432–1443. [PubMed: 26549457]
37. Maraskovsky E, O'Reilly LA, Teepe M, Corcoran LM, Peschon JJ, Strasser A. Bcl-2 can rescue T lymphocyte development in interleukin-7 receptor-deficient mice but not in mutant rag-1−/− mice. Cell. 1997; 89:1011–1019. [PubMed: 9215624]
38. Schmitt TM, Zuniga-Pflucker JC. Induction of T cell development from hematopoietic progenitor cells by delta-like-1 in vitro. Immunity. 2002; 17:749–756. [PubMed: 12479821]
39. Hadeiba H, Lahl K, Edalati A, Oderup C, Habtezion A, Pachynski R, et al. Plasmacytoid dendritic cells transport peripheral antigens to the thymus to promote central tolerance. Immunity. 2012; 36:438–450. [PubMed: 22444632]
40. Heng TS, Painter MW, Immunological Genome Project C. The Immunological Genome Project: networks of gene expression in immune cells. Nat Immunol. 2008; 9:1091–1094. [PubMed: 18800157]
41. Miller JP, Izon D, DeMuth W, Gerstein R, Bhandoola A, Allman D. The earliest step in B lineage differentiation from common lymphoid progenitors is critically dependent upon interleukin 7. J Exp Med. 2002; 196:705–711. [PubMed: 12208884]
42. Yang GX, Lian ZX, Kikuchi K, Moritoki Y, Ansari AA, Liu YJ, et al. Plasmacytoid dendritic cells of different origins have distinct characteristics and function: studies of lymphoid progenitors versus myeloid progenitors. J Immunol. 2005; 175:7281–7287. [PubMed: 16301633]
43. Kamath AT, Henri S, Battye F, Tough DF, Shortman K. Developmental kinetics and lifespan of dendritic cells in mouse lymphoid organs. Blood. 2002; 100:1734–1741. [PubMed: 12176895]
44. Nitta T, Ohigashi I, Nakagawa Y, Takahama Y. Cytokine crosstalk for thymic medulla formation. Curr Opin Immunol. 2011; 23:190–197. [PubMed: 21194915]
45. Williams JA, Zhang J, Jeon H, Nitta T, Ohigashi I, Klug D, et al. Thymic medullary epithelium and thymocyte self-tolerance require cooperation between CD28-CD80/86 and CD40-CD40L costimulatory pathways. J Immunol. 2014; 192:630–640. [PubMed: 24337745]
46. Schlenner SM, Madan V, Busch K, Tietz A, Laufle C, Costa C, et al. Fate mapping reveals separate origins of T cells and myeloid lineages in the thymus. Immunity. 2010; 32:426–436. [PubMed: 20303297]
47. Gendron S, Boisvert M, Chetoui N, Aoudjit F. Alpha1beta1 integrin and interleukin-7 receptor up-regulate the expression of RANKL in human T cells and enhance their osteoclastogenic function. Immunology. 2008; 125:359–369. [PubMed: 18479350]
48. Lucas B, James KD, Cosway EJ, Parnell SM, Tumanov AV, Ware CF, et al. Lymphotoxin β receptor controls T cell progenitor entry to the thymus. J Immunol. 2016; 197:2665–2672. [PubMed: 27549174]
49. Allman D, Sambandam A, Kim S, Miller JP, Pagan A, Well D, et al. Thymopoiesis independent of common lymphoid progenitors. Nat Immunol. 2003; 4:168–174. [PubMed: 12514733]

50. Laurent J, Bosco N, Marche PN, Ceredig R. New insights into the proliferation and differentiation of early mouse thymocytes. Int Immunol. 2004; 16:1069–1080. [PubMed: 15197172]

51. Poliani PL, Facchetti F, Ravanini M, Gennery AR, Villa A, Roifman CM, et al. Early defects in human T-cell development severely affect distribution and maturation of thymic stromal cells: possible implications for the pathophysiology of Omenn syndrome. Blood. 2009; 114:105–108. [PubMed: 19414857]

52. Notarangelo LD, Gambineri E, Badolato R. Immunodeficiencies with autoimmune consequences. Adv Immunol. 2006; 89:321–370. [PubMed: 16682278]

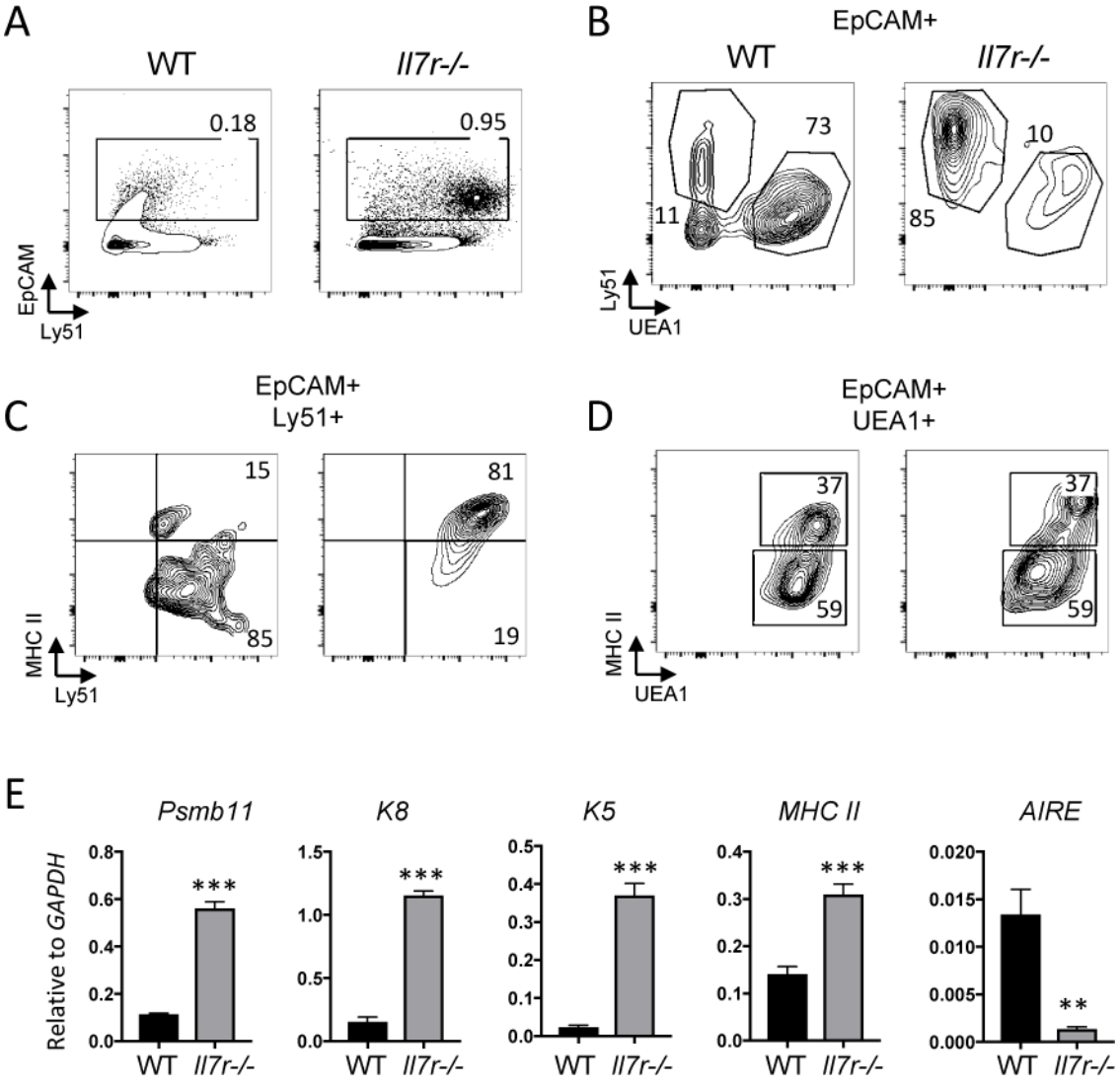

Figure 1.

Defects in thymic epithelial cell subset ratios in the *Il7r*$^{-/-}$ thymus. **A**. Thymus single cell suspensions were made by collagenase digestion and analyzed by flow cytometry. EpCAM staining was used to gate on the TECs. **B**. EpCAM-gated cells were stained with Ly51 to identify cTECs, and UEA-1 to identify mTECs. **C, D**. cTECs (**C**) or mTECs (**D**) were further gated to analyze the expression of Class II MHC as a marker of maturity. Numbers in quadrants indicate percentages. **E**. Whole WT and *Il7r*$^{-/-}$ thymuses were homogenized, RNA was extracted, and first strand cDNA was generated to be used as template for qRT-PCR. The mRNA expression of the cTEC markers *Psbm11* (β5t) and *cytokeratin-8 (K8)*, the mTEC marker *cytokeratin-5 (K5)*, *MHC Class II*, and the mature mTEC marker *AIRE* were measured. All values shown are relative to *GAPDH* levels. Graphs depict means +/− SEM, n=3. Statistical significance was calculated using a t-test; *** p<0.005. Data is representative of at least 2 separate experiments.

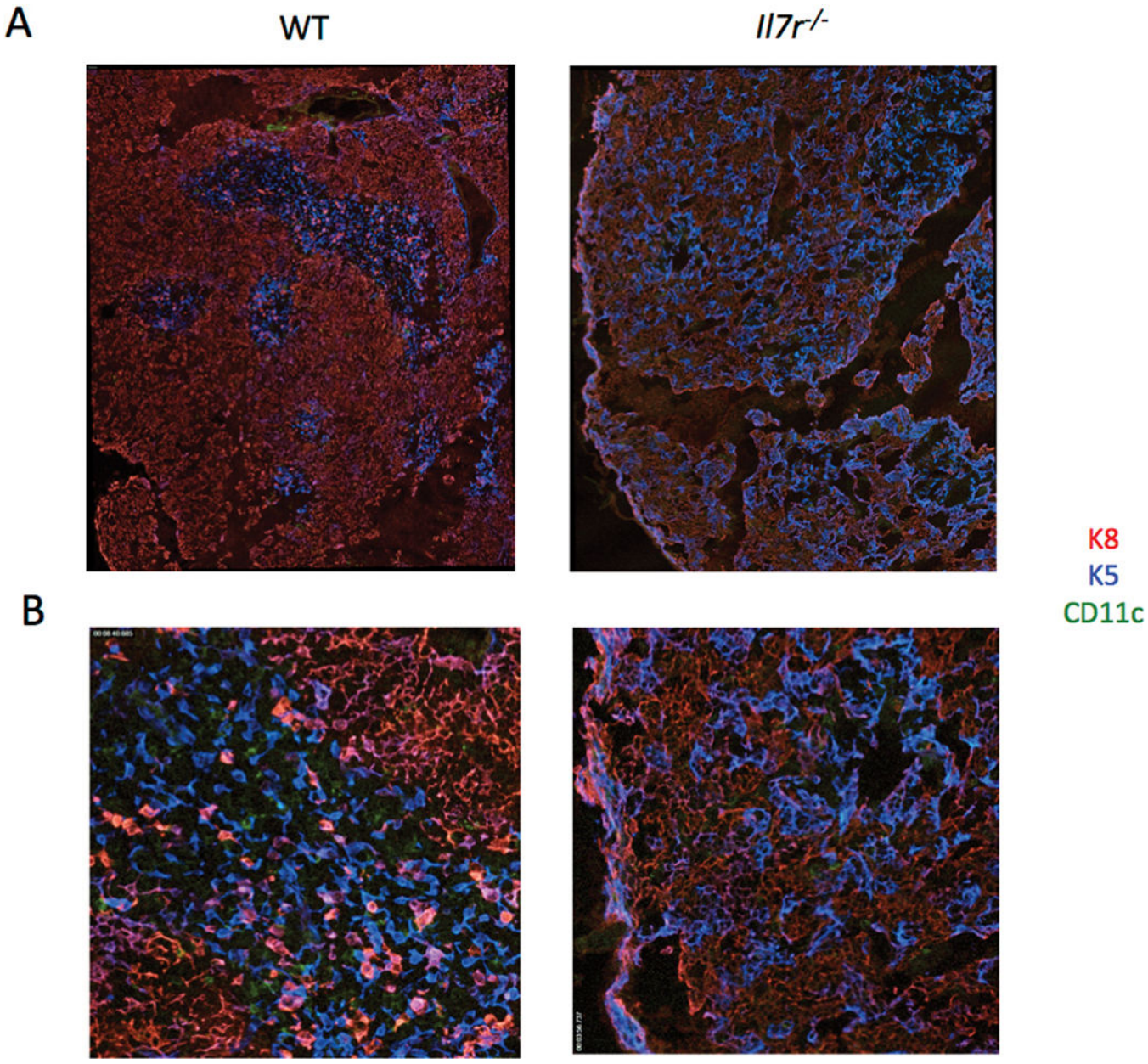

Figure 2.

The *Il7r*$^{-/-}$ thymus has disorganized corticomedullary structure and a paucity of DCs. Thymuses were dissected from WT and *Il7r*$^{-/-}$ mice and snap frozen in OCT freezing media. 10 μm sections were cut and stained with anti-cytokeratin 8 (K8)/anti-rat conjugated to Cy3 (cTECs, red), anti-cytokeratin 5 (K5)/anti-rabbit conjugated to Cy5 (mTECs, blue), and anti-CD11c directly conjugated to FITC (DCs, green). Tiled images were gathered using an Axiovert microscope, shown at either 10X (**A**) or 20X (**B**).

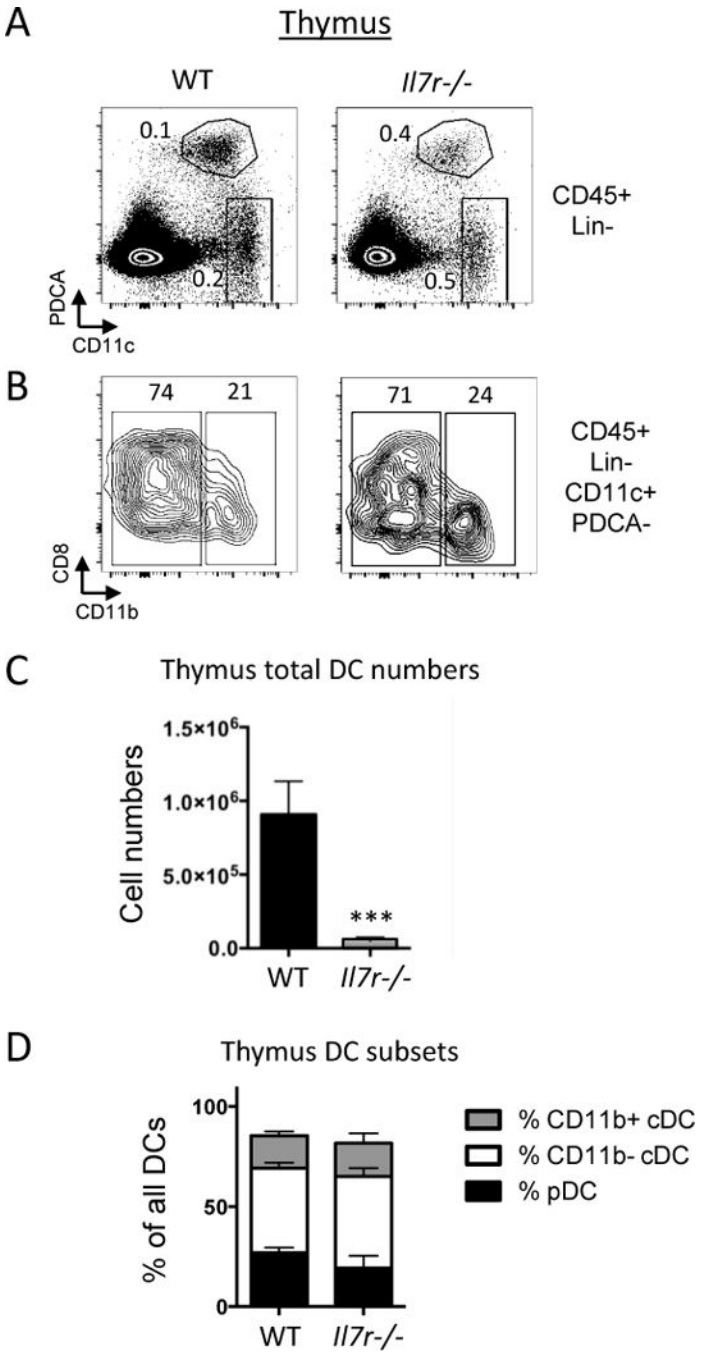

Figure 3.

Marked reduction of thymic DC numbers in *Il7r*$^{-/-}$ mice. WT and *Il7r*$^{-/-}$ mice were analyzed at 4.5–5.5 weeks of age. **A**. Gates used to analyze pDCs and cDCs. Cells were first gated on the lineage (Lin)-negative, DAPI^{-}, CD45^{+} populations, where Lin=Dx5, NK1.1, F4/80, CD3ε, TCRγδ, TCRβ, CD19, Ter119. Within this gate, two populations were analyzed: pDCs (CD11c^{int}, PDCA-1^{+}) and cDCs (CD11c^{high}, PDCA-1^{-}). **B**. To further differentiate between cDC subsets, cells within the cDC gate were analyzed for expression of CD11b and CD8α. CD8α staining was consistently heterogeneous within the CD11b^{-}

population. Numbers within the quadrants represent percentages. **C**. Total numbers of DCs per thymus, as calculated from manual counting from single cell suspensions multiplied by the percentages of $CD45^{+}Lin^{-}CD11c^{+}$ cells as determined by Flow Jo. **D**. Ratios of the three DC subsets out of all DCs were calculated by taking the numbers of thymic pDCs, $CD11b^{+}$ cDCs, and $CD11b^{-}$ cDCs per thymus and dividing by the total number of DCs. n=4. ***$p<0.005$. Data is representative of three separate experiments.

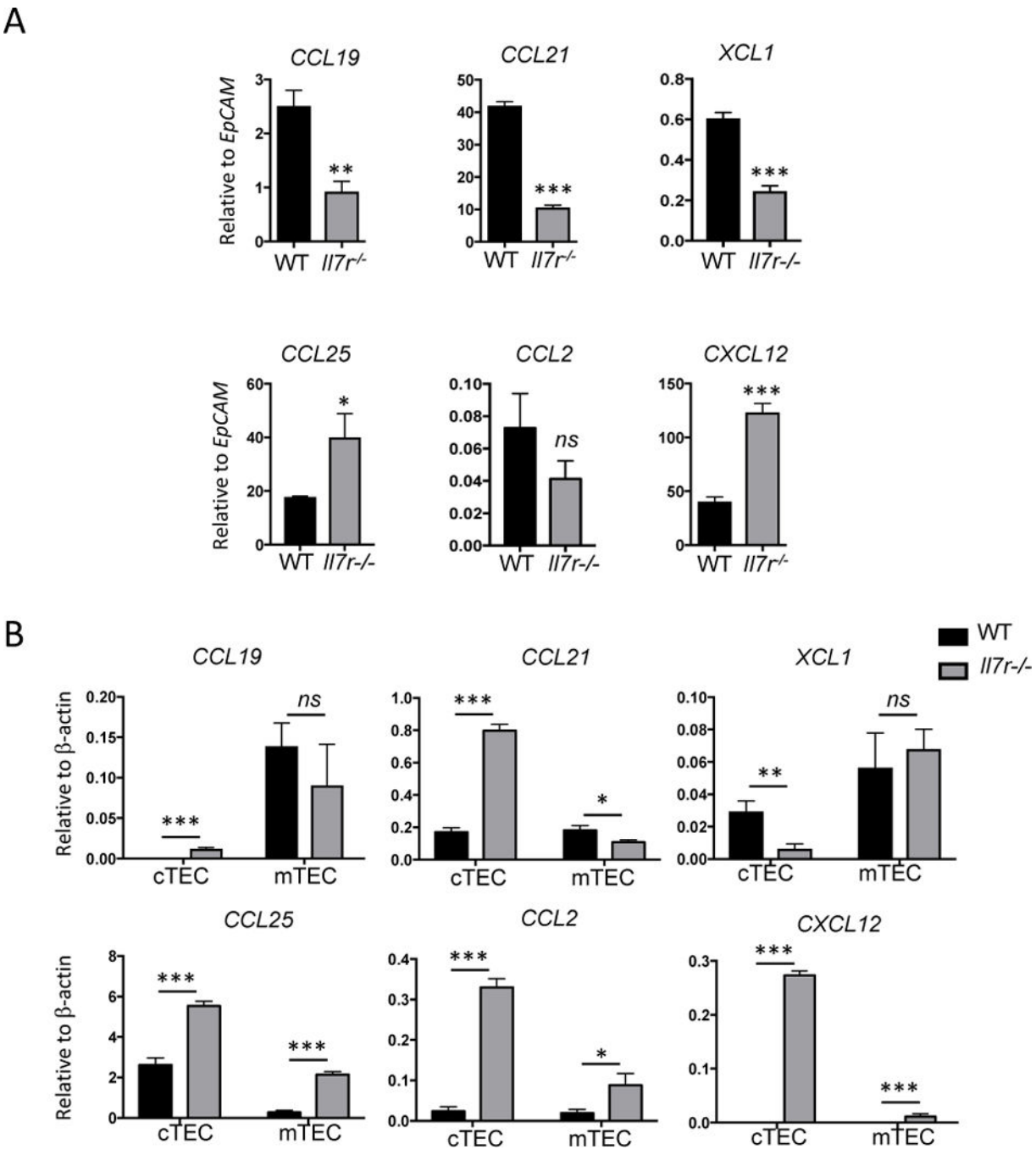

Figure 4.

Perturbation in chemokine expression in the *Il7r*$^{-/-}$ thymus. **A**. Whole homogenized thymus was used as a template for qRT-PCR to measure the amount of chemokine mRNA produced in the adult WT versus *Il7r*$^{-/-}$ thymus. To account for the 5-fold greater number of TECs in the *Il7r*$^{-/-}$ thymus versus the WT thymus, results were normalized to *EpCAM* mRNA levels. **B**. TECs were sorted based on expression of EpCAM, and Ly51 (cTECs) or UEA-1 (mTECs). cDNA was generated from sorted TEC subsets and used as template for qRT-PCR. n=3. Values were normalized to β-actin mRNA levels. Data is representative of at least

two separate experiments. Graphs depict means +/− SEM. Statistical significance was calculated using a t-test; *** $p<0.005$, **$p<0.01$, *$p>0.05$.

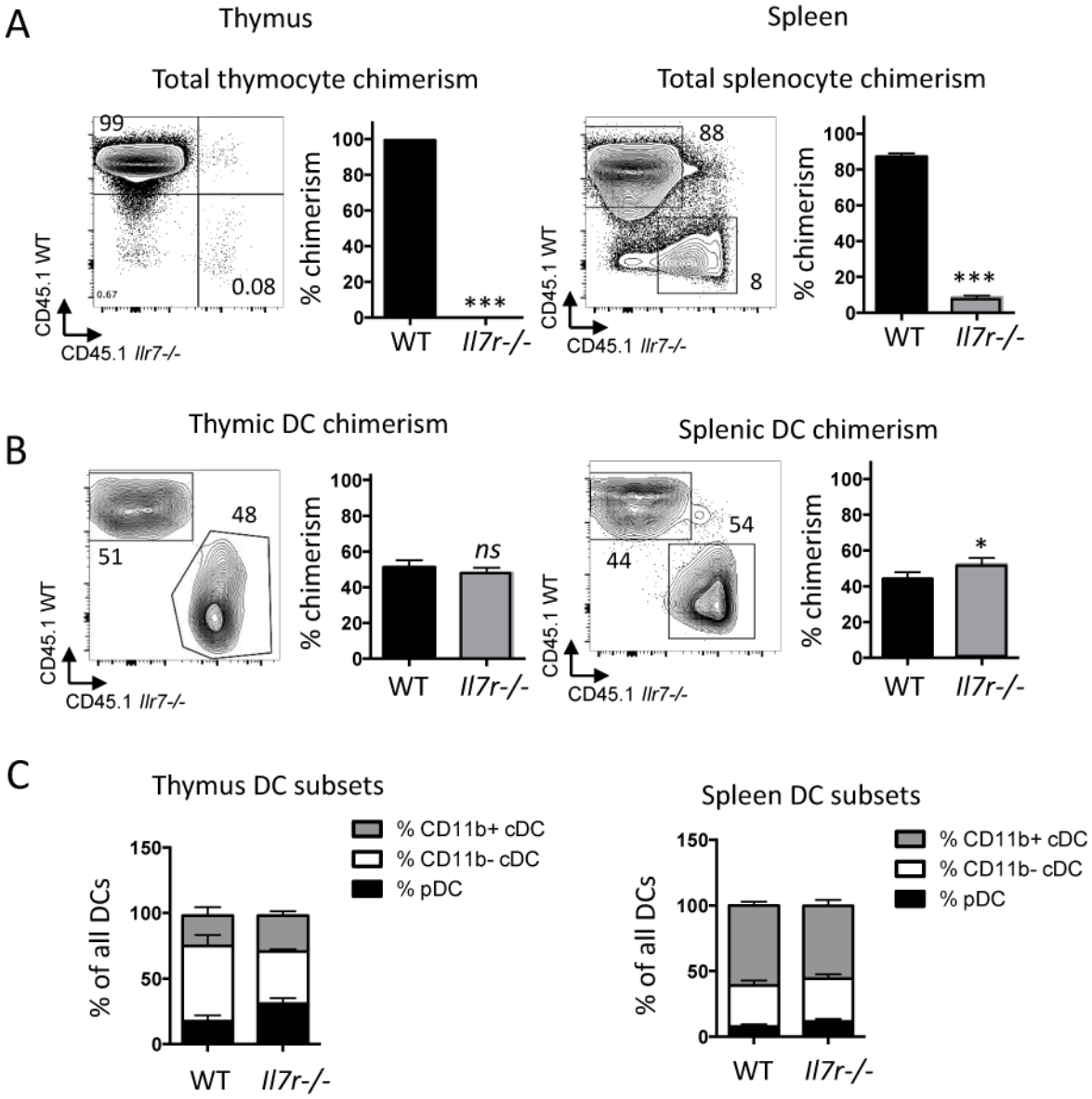

Figure 5.

Contribution of *Il7r*$^{-/-}$ bone marrow-derived cells to thymic and splenic DCs in mixed radiation chimeras. Lethally irradiated CD45.1^{+} × CD45.2^{+} F1 hybrid mice were reconstituted with a 1:1 mix of CD45.1^{+}WT:CD45.2^{+} *Il7r*$^{-/-}$ BM. Tissues were analyzed three weeks later. **A**, **B**. Chimerism in whole thymus (**A**) or in DCs (**B**) were calculated as the percentage contribution from *Il7r*$^{-/-}$ versus WT BM derived cells as assessed by CD45.1 (WT) or CD45.2 (*Il7r*$^{-/-}$) expression, in thymus (left) or spleen (right). The graph depicts the mean +/− SEM. Numbers in the quadrants indicates percentages. **C**. Ratios of pDCs, CD11b^{-} cDCs, and CD11b^{+} cDC subsets among all DCs in the thymus (left) or spleen (right), calculated by dividing the number in each subset per organ by the total number of DCs. Statistical significance was calculated using a t-test. ***p<0.005, *p<0.05, *ns*=non-significant. n=4. Data is representative of two separate experiments.

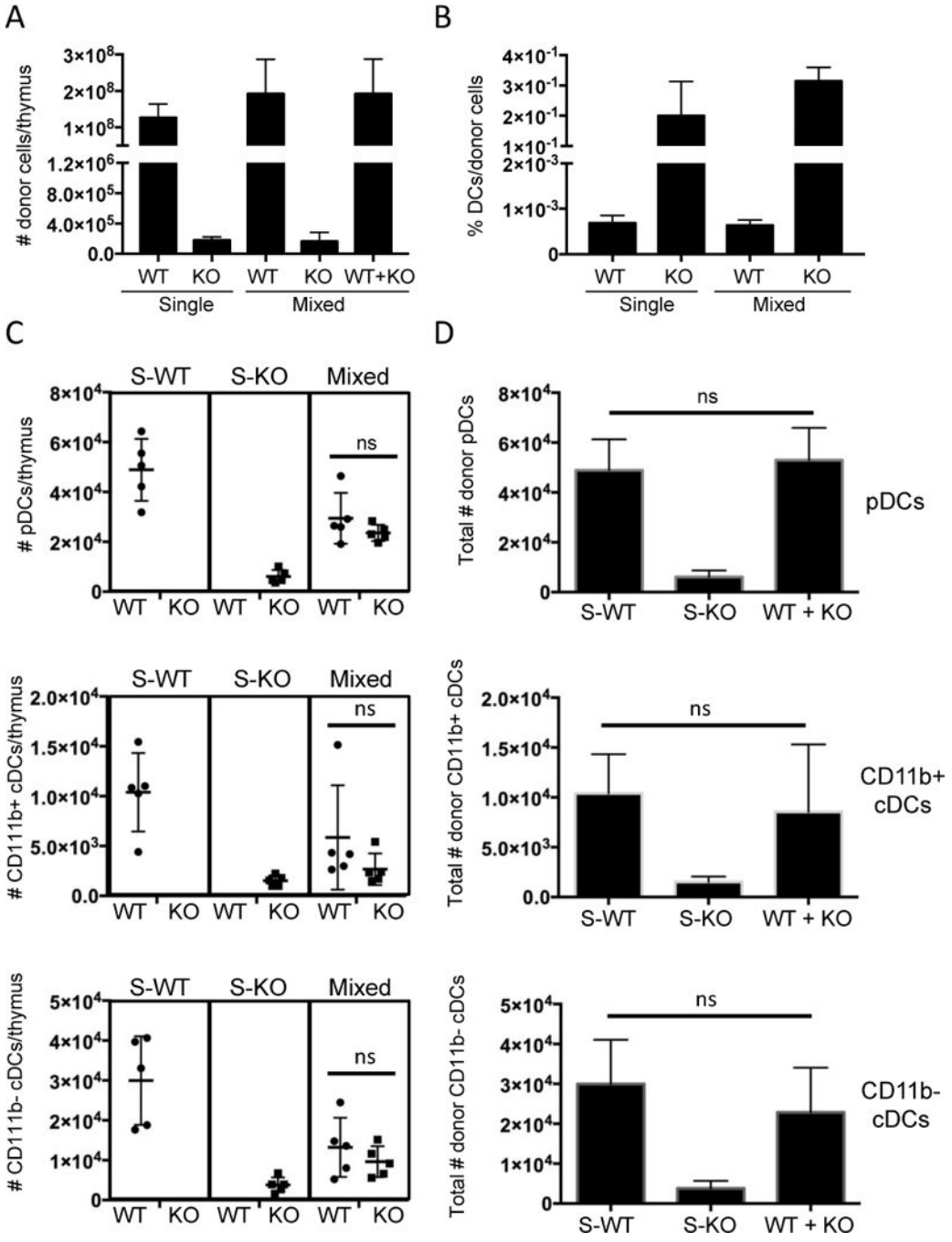

Figure 6.

Increase of *Il7r*$^{-/-}$ donor-derived thymic DC cell numbers by the provision of WT donor cells. Lethally irradiated CD45.1^{+} × CD45.2^{+} F1 hybrid mice were reconstituted with whole BM from CD45.1^{+} WT mice ("S-WT"), CD45.2^{+} *Il7r*$^{-/-}$ ("S-KO") mice or a 1:1 mix of each (Mixed). The thymus was analyzed by manual counting and flow cytometry three weeks later. **A**. Numbers of CD45^{+} donor cells of the indicated genotypes per thymus in the single and mixed chimeras. **B**. Percentages of total DCs within the total donor populations of the indicated genotypes (WT or KO) in the single and mixed chimeras. **C**. Numbers of

pDCs, CD11b^{+} cDCs, and CD11b^{-} cDCs per thymus of the indicated genotypes (indicated below the graph) in the single and mixed chimeras (indicated above the graph). **D**. Comparison of the sum of WT and KO cell numbers in the mixed chimeras to the WT or KO cell numbers in the single chimeras. The graphs depict the mean +/− SEM. Statistical significance was calculated using a t-test. *ns*=non-significant, n=5. Data is representative of two separate experiments.